Superalloys 2008
Roger C. Reed, Kenneth A. Green, Pierre Caron, Timothy P. Gabb, Michael G. Fahrmann, Eric S. Huron and Shiela A. Woodard
TMS (The Minerals, Metals & Materials Society), 2008

Fatigue Crack Initiation in Nickel-based Superalloy René 88 DT at 593 °C

Jiashi Miao[1], T. M. Pollock[1], J. W. Jones[1]
[1]Department of Materials Science and Engineering, University of Michigan, Ann Arbor, MI-48109, USA

Keywords: Fatigue, Nickel-based superalloy, Crack initiation, Crystallographic facet, Annealing twin boundary

Abstract

Fatigue crack initiation in the polycrystalline nickel-based superalloy, René 88 DT, was investigated at 593 °C in air using an ultrasonic fatigue testing instrument. Within the testing stress range of 500 - 760MPa, all fatigue failures initiated from internal regions. Large crystallographic facets were observed at the crack initiation sites in most failed fatigue samples. Critical microstructure features controlling fatigue crack initiation and the early stage of small crack growth were identified by the combination of serial sectioning, orientation imaging microscopy (OIM) and quantitative fractographic analysis. Large crystallographic facets at crack initiation sites were formed in regions close to Σ 3 annealing twin boundaries within favorably oriented large grains. The facet planes are parallel to Σ 3 annealing twin boundaries and are of {111} type. Cyclic deformation substructures were studied by transmission electron microscopy. At the low cyclic stresses and long lives examined, fatigue failure at 593°C is controlled by strain localization in large, favorably oriented grains and subsequent propagation of small cracks through neighborhoods of favorably oriented grains. Annealing twin boundaries, prevalent in the microstructure, appear to be important in cyclic strain localization.

Introduction

Polycrystalline nickel-based superalloys are extensively used in the aerospace and power-generation industries, owing to their excellent combination of mechanical and environmental properties at elevated temperature. For polycrystalline nickel-based superalloys, fatigue is one of the most important properties, often limiting the overall service life. Future engine applications require engine components that can operate safely up to 10^9 cycles [1]. In the very high cycle regime, most fatigue life is believed to be consumed by fatigue crack initiation processes [2].

Fatigue crack initiation and damage accumulation in nickel-based superalloys depend on both intrinsic microstructure and extrinsic testing conditions such as temperature, loading stress and environment [3]. Intrinsic microstructure associated with fatigue crack initiation includes: metallurgical defects such as inclusions and pores, and microstructure heterogeneities such as grain size inhomogeneity, microtexture and large-angle grain boundaries. Metallurgical defects are mainly responsible for fatigue failures under high loading stresses and in the low cycle regime [4, 5]. In studying elevated temperature fatigue behavior of Udimet 700 alloy, Organ and Gell [6] found that fatigue cracks initiated from small inclusions located at grain boundaries and at intersections of annealing twin boundaries. Twin boundaries were reported to be important sources for fatigue cracking in Udimet 700 alloy at room temperature [7]. Fatigue cracks were observed to initiate at the surface in large grains in Waspaloy at room temperature [8]. Li et al. [9] found that large grains and favorably orientated local texture might promote fatigue crack initiation in IN100 nickel-base superalloy. Recently, Davidson et al. [10, 11] reported that in Waspaloy at 20°C fatigue cracks initiated from clusters of surface grains, termed supergrains, that were favorably orientated for slip transmission across grain boundaries.

Research on fatigue crack initiation in nickel-based superalloys has primarily concentrated in the low cycle regime ($<10^5$ cycles) or high cycle regime ($<10^7$ cycles). To date, few studies have been devoted to the investigation of fatigue crack initiation mechanisms in polycrystalline nickel-based superalloys in the very high cycle regime ($>10^7$ cycles). The main difficulty of investigating very high cycle fatigue behavior using conventional frequency fatigue instruments is the long time required to achieve very high cycle counts. Recent developments in ultrasonic fatigue techniques offer a powerful and promising method to study very high cycle fatigue behavior in an efficient way [12]. In the current study, the fatigue crack initiation behavior in a polycrystalline nickel-based superalloy, René 88 DT, was examined up to 10^9 cycles using an ultrasonic fatigue testing instrument. Critical microstructure features that contributed to fatigue crack initiation and microstructure barriers to the early stages of small crack growth were systematically characterized by quantitative fractographic analysis, serial sectioning and orientation imaging microscopy. By combining these observations with the results of TEM deformation substructure analysis, possible cyclic strain localization and fatigue crack nucleation mechanisms in this alloy at 593 °C are proposed.

Material and Experimental Procedures

Microstructure characterization

The material tested in this study is a polycrystalline nickel-based superalloy, René 88DT. The alloy was prepared by advanced powder metallurgy techniques and has a nominal composition of 13Co, 16Cr, 4Mo, 4W, 2.1Al, 3.7Ti, 0.7Nb, 0.03C, 0.015%B (weight percent) [13]. The microstructure of the alloy consists of a γ matrix and two populations of gamma prime (γ′) precipitates. Figure 1 shows the typical morphology of secondary and tertiary γ′ within a γ grain. There is no primary γ′ in the microstructure due to the supersolvus heat treatment. The size of the secondary γ′ phase is about 100-200 nm, while tertiary γ′ sizes are several nm. Crystallographic features associated with γ grains were quantitatively characterized by orientation imaging microscopy. Figure 2(a) is an inverse pole figure map based on a large area OIM scan. The corresponding pole figures indicate that there is very weak texture in the microstructure. The grain boundary character distribution within this alloy is shown in Figure 2(b). The length fraction of Σ3 grain boundary is about 0.58, while the total fraction of $\Sigma 3^n$ (n>1) grain boundary in grain interface length is only about 0.08. The distribution of grain size is shown in Figure 3 The average grain size of the alloy, excluding annealing twin boundaries, is about 26μm. A low fraction of large grains on the order of two to five times of the average grain size exists in the microstructure.

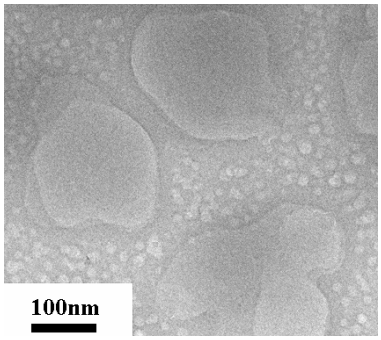

Figure 1. The morphology of γ′ precipitates within a γ grain.

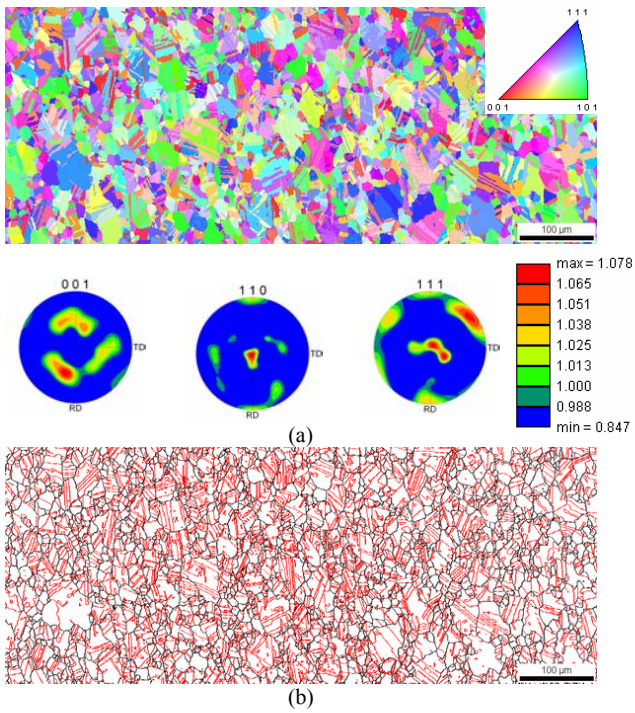

Figure 2. Crystallographic features of γ grains in René 88DT, (a) orientation map and corresponding pole figures, (b) reconstructed grain boundary map, (Black lines represent random grain boundaries, red lines represent annealing twin boundaries).

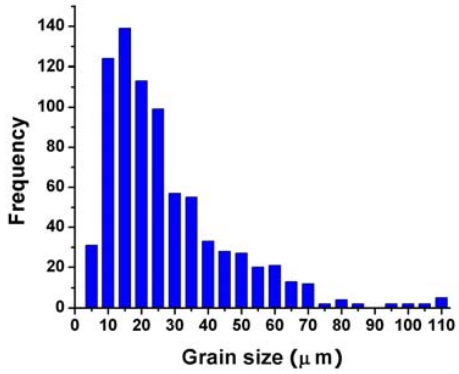

Figure 3. Grain size distribution

Experimental Procedures

Ultrasonic fatigue testing was conducted at a resonance frequency of approximately 20 kHz, under a positive stress ratio R =0.05 at 593°C in air [14, 15]. Cylindrical specimens with a gage diameter of 5mm and gage length of 16mm were used in this study. Fatigue specimens were machined using low stress grinding. Each ultrasonic fatigue specimen was electropolished to minimize the effect of residual stress. Ultrasonic fatigue loading was applied in pulsed mode with pulses of 500 ms separated by pauses of 900 ms. The spatial orientation of crystallographic facets at crack initiation sites was determined using stereology and three dimensional fracture surface reconstruction methods [15]. The crystallographic orientations of grains at and around crack initiation sites were revealed by combining orientation imaging microscopy (OIM) and metallographic serial sectioning. The OIM studies were performed using TSL OIM software on a FEG XL30 SEM. Disc samples for TEM studies were sectioned perpendicular to the loading axis from the gage section of the failed fatigue specimens. The samples were mechanically polished to a thickness of approximately 100 μm, and further thinned by twin jet polishing in a solution of 68% methanol, 10% perchloric acid, 9% distilled water and 13% butyl cellosolve under conditions of -35°C, 20V and 50mA. Observations of the deformation substructures were conducted using a JEOL 2010F TEM operated at 200 KeV.

Results and Discussion

S-N curve

The ultrasonic fatigue stress-life curve for René 88 DT at 593°C is shown in Figure 4 [15]. The loading stresses are in the range of 500 - 760MPa, which are much lower than the yield strength of the alloy, which is approximately 940MPa at 593°C [16]. Fatigue failures were observed in this alloy for lifetimes beyond 10^8 cycles. The variability of fatigue life increases with the decrease

of cyclic stress and exceeds two orders of magnitude at σ_{max} = 600MPa.

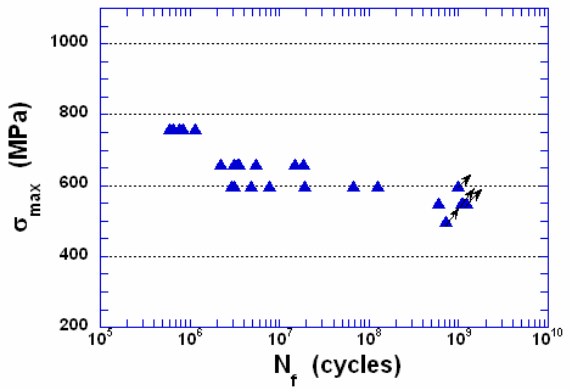

Figure 4. S-N data of Rene 88 DT at 593°C (Arrows indicate runouts).

Critical microstructural features associated with fatigue crack initiation

SEM fractographic analysis indicated that all fatigue failures have internal origins. Most fatigue crack initiation sites have large crystallographic facets with no large metallurgical defects such as inclusions or pores observed. The sizes of facets at crack initiation sites are much larger than the mean grain size of this alloy and on the order of the largest grains observed in the microstructure. According to their spatial geometry, large crystallographic facets at crack initiation sites can be grouped into two types: single plane facet and chevron shape facet [15]. Figure 5 shows the example of two kinds of crystallographic facets. The chevron facet is the dominant type facet. By using three dimensional reconstruction and quantitative fracture surface analysis techniques, the spatial orientation of several chevron facets at crack initiation sites were calculated and are listed in Table I. The results indicate that chevron shape facets at crack initiation sites have similar geometrical configuration; both facet planes within a chevron facet are oriented close to 45 degrees with respect to the loading axis. Thus, both facet planes within the chevron facet are close to maximum resolved shear stress orientation.

The internal origin of fatigue cracks makes it more difficult to directly characterize critical microstructure features controlling fatigue crack initiation and the early stage of fatigue crack growth. Therefore, metallographic serial sectioning was used to expose such critical microstructure features at the crack initiation sites. In order to collect the detailed microstructure just beneath the crystallographic facets, serial sectioning parallel to the loading axis was performed. The advantage of this sectioning method is that three-dimensional information of microstructure and fracture surface morphology can be simultaneously examined. Failed samples were mounted in resin to protect the fracture surface from damage during sectioning. Matching halves of the failed samples were mounted and sectioned. In this way, microstructure just below and above the crystallographic facets can be revealed and characterized. The sectioning depth was well controlled by using pyramidal Vickers hardness indents in order to section directly through the crystallographic facet at crack initiation sites. Microstructure information beneath the fracture surface was collected on the sectioning planes by using OIM.

Two specimens that failed at 600MPa were selected for studying critical microstructure information. The fracture surfaces of the two samples before serial sectioning are shown in Figure 5.

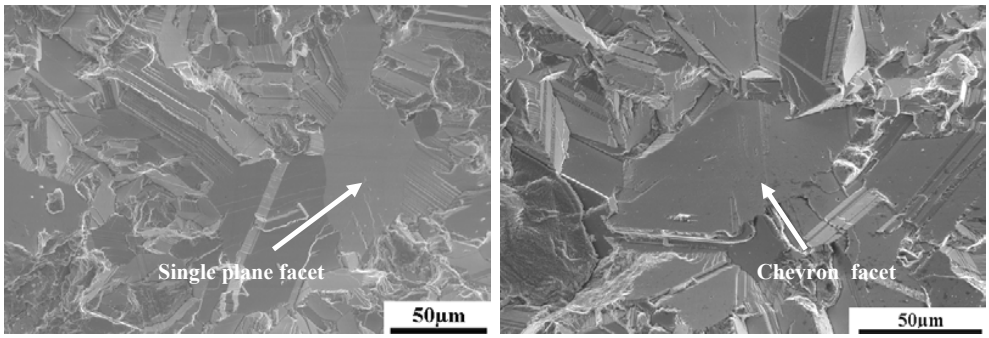

(a) (b)

Figure 5. Two types of large crystallographic facet at crack initiation site, (a) single plane facet (σ_{max}= 600MPa, N_f = 3.16x10^6) (b) chevron shape facet (σ_{max}=600MPa, N_f=1.90x10^7).

Table I. Spatial orientation of crystallographic facets at crack initiation sites with chevron shape.

Specimen No.	1		2		3		4		5		6	
Angles between loading axis and two facet plane normal (degrees)	43	41	43	47	40	44	42	44	42	44	46	53
Angle between two facet planes (degrees)	40		37		32		42		35		41	

Figure 6(a) shows the serial sectioning plane directly cut through the single plane facet at the crack initiation site. Microstructural information just beneath the fracture surface was collected using OIM on the sectioning planes on both halves of the failed sample. Figure 6(b) shows a matched large area OIM map. The orientation information for the crack initiation grain is illustrated in Figure 6(c). Figure 6(d) is the corresponding reconstructed grain boundary map. The crystallographic facet was formed within a large grain. Large size grains can provide long slip lengths that favor cyclic strain localization. Within the large crack initiation grain there is a stack of parallel annealing twins. The facet plane was formed in the region close to a twin boundary and intersected the step of the annealing twin boundary as indicated in Figure 6(c). The facet plane is parallel to Σ 3 twin boundary indicating it is of {111} type.

Figure 7 (a) shows the fracture surface of the second sample after serial sectioning. The metallographic sectioning plane cut through the chevron facet at the crack initiation site. The microstructure details of the crack initiation grain were revealed by an inverse pole figure map (Figure 7(b)) and a reconstructed grain boundary map (Figure 7(c)) respectively. Facet planes, A and B of the chevron facet, as marked in Figure 7(c), are within one large grain. Microstructural features of the crack initiation grain are very similar to those of the first sample. There is a stack of parallel annealing twins within the large crack initiation grain. The facet plane A is formed at the twin step and near and parallel to a Σ 3 twin boundary.

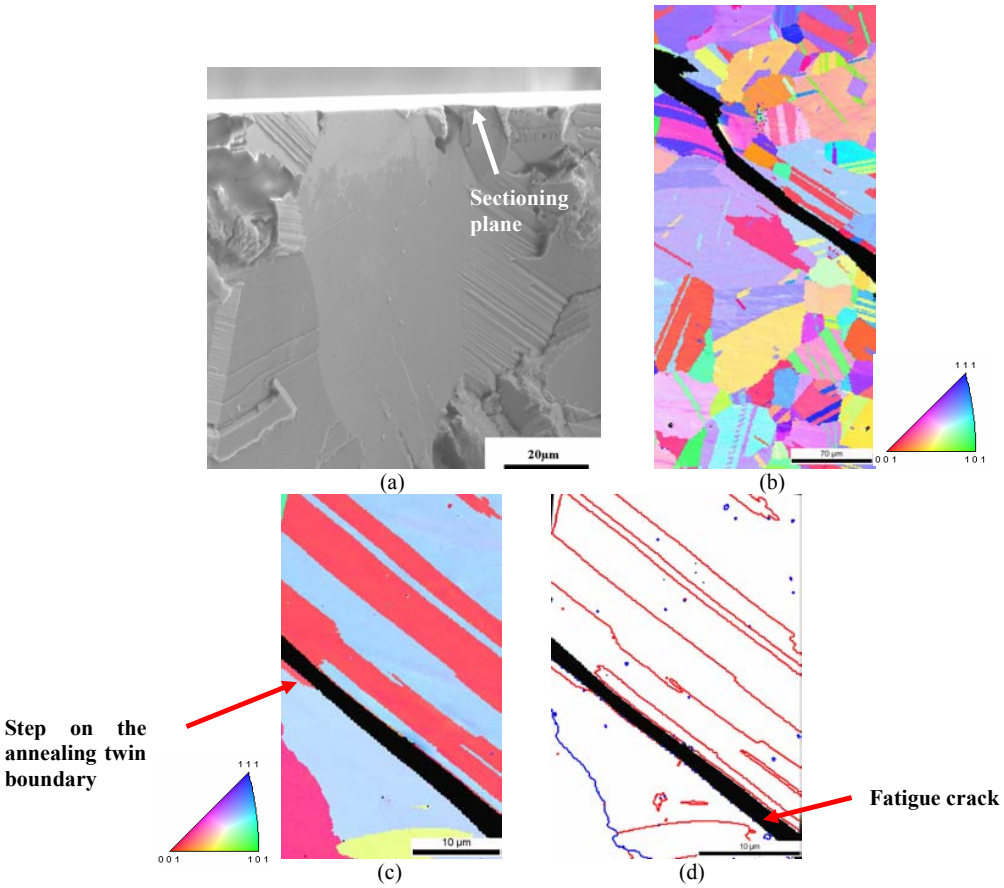

Figure 6. Microstructural features of the crack initiation grain, (a) metallographic sectioning through the single plane facet at crack initiation site, (b) large area OIM maps of matching halves, (c) inverse pole figure map of the crack initiation grain. (d) reconstructed grain boundary map of the crack initiation grain. (Blue lines represent random grain boundaries, red lines represent Σ 3 annealing twin boundaries).

The metallographic serial sectioning method also revealed the formation of microcracks in internal grains not associated with the fatal crack. The SEM image in Figure 8(a) shows a microcrack formed in a large size internal grain. The detailed structure of the grain was identified using OIM. Figure 8(b) is the reconstructed grain boundary map overlayed with OIM image quality map. The position of the crack is highlighted on the images. The microcrack was formed in the region close to a Σ 3 annealing twin boundary. Room temperature fatigue testing in this alloy at low stresses also revealed that microcracks initiated near and parallel to annealing twin boundaries in surface large grains, as described above for internal initiation at 593°C. Similarly, fatigue crack initiation in the region close to annealing twin boundaries has been observed in other FCC materials [17, 18]. Annealing twin boundaries are thought to be important locations for cyclic strain localization and fatigue crack initiation in FCC materials due to elastic anisotropy between the twin and matrix [19].

After fatigue crack initiation, it is reasonable to assume that surrounding microstructural barriers such as grain boundaries will determine if the small crack can continue to propagate to a critical length for eventual failure. As indicated in Figure 7(c), between crystallographic facet plane A and B, there is another Σ 3 grain boundary. Within the chevron facet, the twist angle between two facet planes is zero. Additionally, both facet planes are {111} slip planes oriented for maximum resolved shear stress. Such a configuration satisfies the conditions for transmission of slip through grain boundaries [20]. This favorable orientation relationship favors the propagation of the crack through the Σ 3 twin boundary, which results in the chevron facets observed at initiation sites.

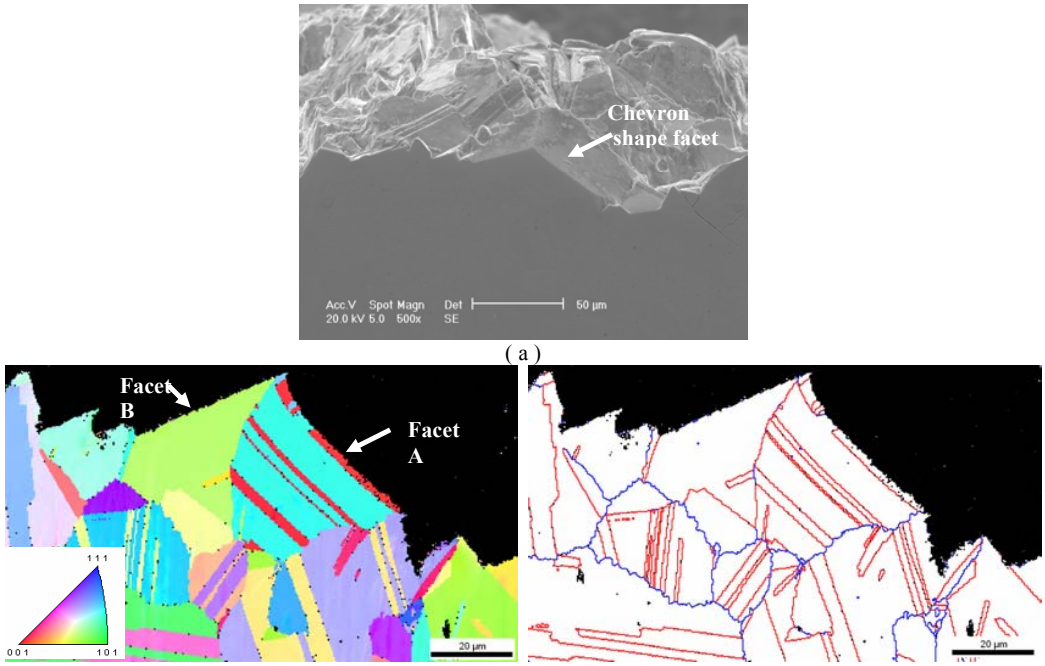

Figure 7. Microstructure details of the crack initiation grain at the crack initiation site, (a) metallographic sectioning through the chevron facet, (b) orientation map of the chevron facet, (c) reconstructed grain boundary map (Blue lines represent random grain boundaries, red lines represent Σ 3 annealing twin boundaries).

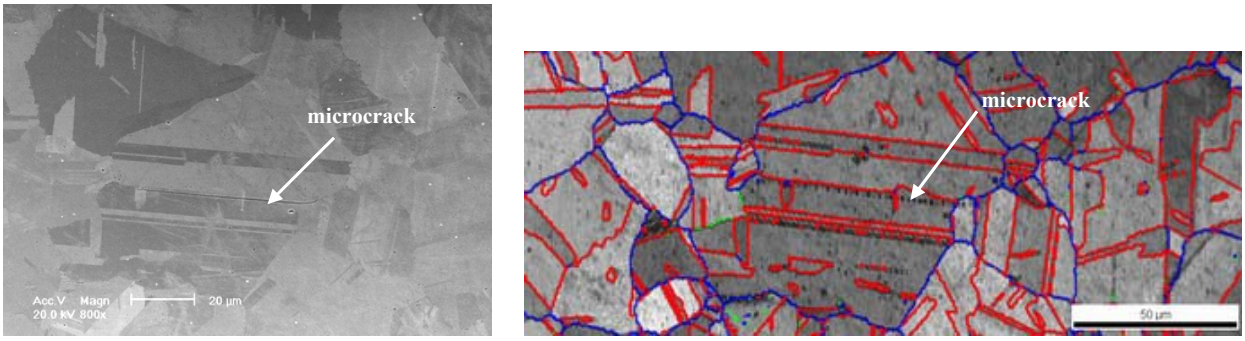

Figure 8. Formation of microcrack in the region close to a Σ3 annealing twin boundary, (a) SEM images, (b) reconstructed grain boundary overlayered by image quality map.(The blue lines represent random grain boundary, red lines represent Σ3 annealing twin boundary , and green lines represent small angle grain boundaries (angle <10°).

Deformation substructure analysis

For the fatigue lifetimes examined in this study, the cyclic loading stresses are much lower than the overall yield strength of the alloy. Most grains within the samples deform elastically. Under these conditions, cyclic plastic deformation and the accumulation of fatigue damage are expected to occur at microstructure heterogeneities or local stress concentrators. The magnitude of stress concentration and strain localization varies with different microstructure heterogeneities. Therefore, plastic deformation within the specimen should be inhomogeneous and vary with grain size, grain orientation and orientation of surrounding grains.

To examine the nature of cyclic strain localization and damage accumulation mechanisms under such low cyclic loading stresses, TEM foils were removed from a fatigued specimen that failed at 5.85×10^8 cycles at 550MPa. Transmission electron microscopy observations indicate that only a very small portion of the grains experienced plastic deformation during fatigue testing. Figure 9(a) shows that slip bands were formed along an annealing twin boundary. Figure 9(b) shows a slip band was formed at or near a step in an annealing twin boundary. Llane and Laird [21] found that twin boundaries, and especially, discontinuities on twin boundaries are significant stress raisers in FCC metals and can promote strain localization and subsequent persistent slip band formation in high cycle fatigue.

Dislocations and stacking faults were observed along annealing twin boundaries near the intersection of two annealing twins in Figure 10. However, far away from twin intersections, in Figure 10(c), few dislocations are observed. Furthermore, cyclic strain localization in large grains in the form of discrete slip bands, an example of which is shown in Figure 11, was often observed in the present study near twins, which is consistent with the findings of previous research [21].

Although annealing twin boundaries are prevalent in the microstructure of the alloy, TEM observations indicate that slip bands form only at a small fraction of twin boundaries and their discontinuities or configurations. Based on the analysis of microstructure features associated with the crack initiation site observed here, a possible explanation for the observation of such limited slip band formation is that twin boundaries alone may not provide sufficient stress concentration for cyclic strain localization to develop under very low stresses. Rather, the presence of a large grain or grain cluster with favorable orientation may be necessary to promote strain localization and subsequent propagation of small fatigue cracks.

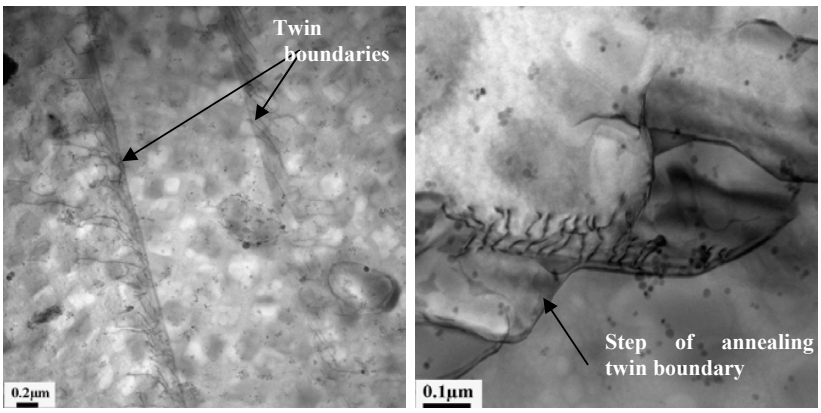

Figure 9. Slip bands formed at annealing twin boundaries, (a) along an annealing twin boundary, (b) at the step of an annealing twin boundary.

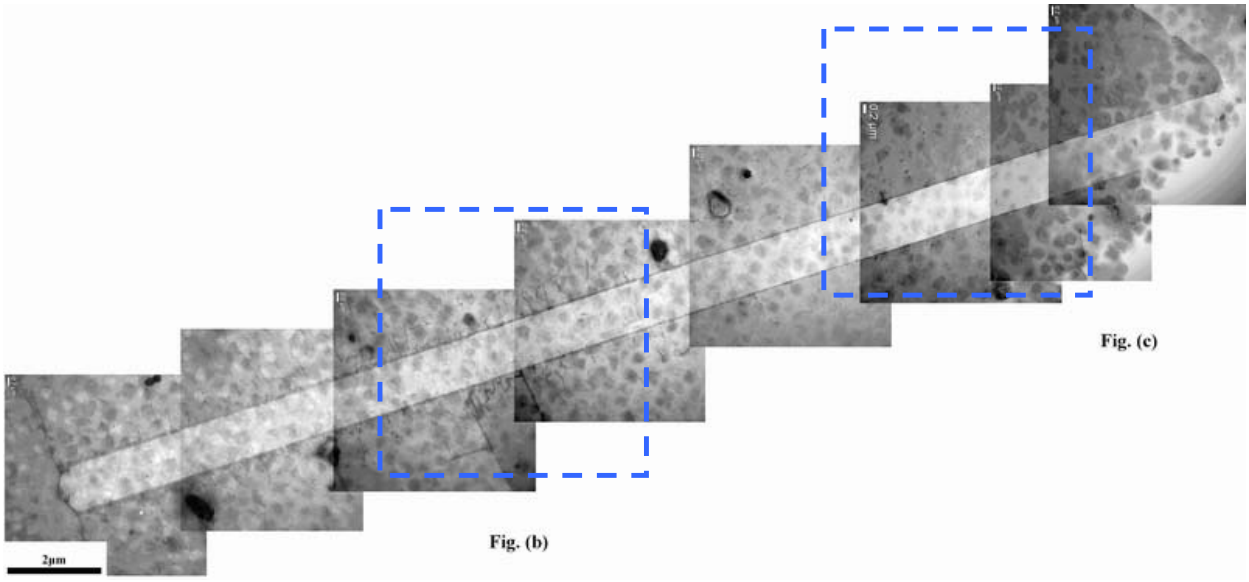

(a)

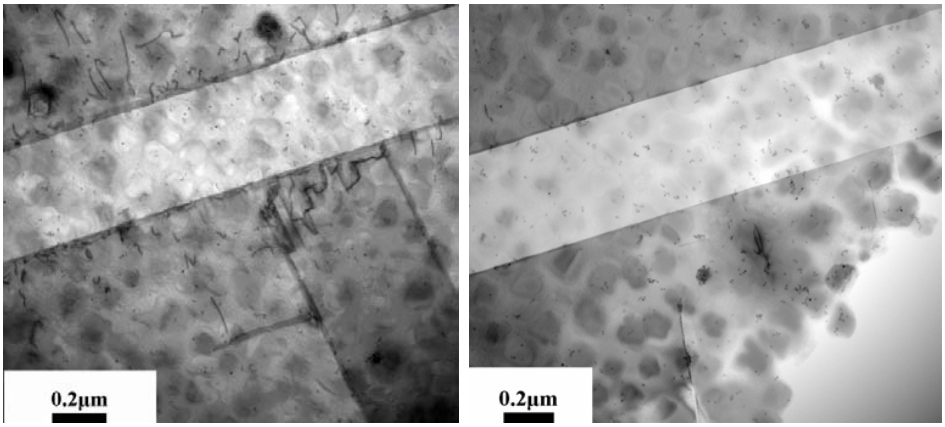

(b) (c)

Figure 10. Dislocations and stacking faults originated at the region close to twin boundaries at the twin intersection, (a) overview of twin intersection, (b) high magnification view of the twin intersection area, (c) high magnification view of area far away from twin intersections.

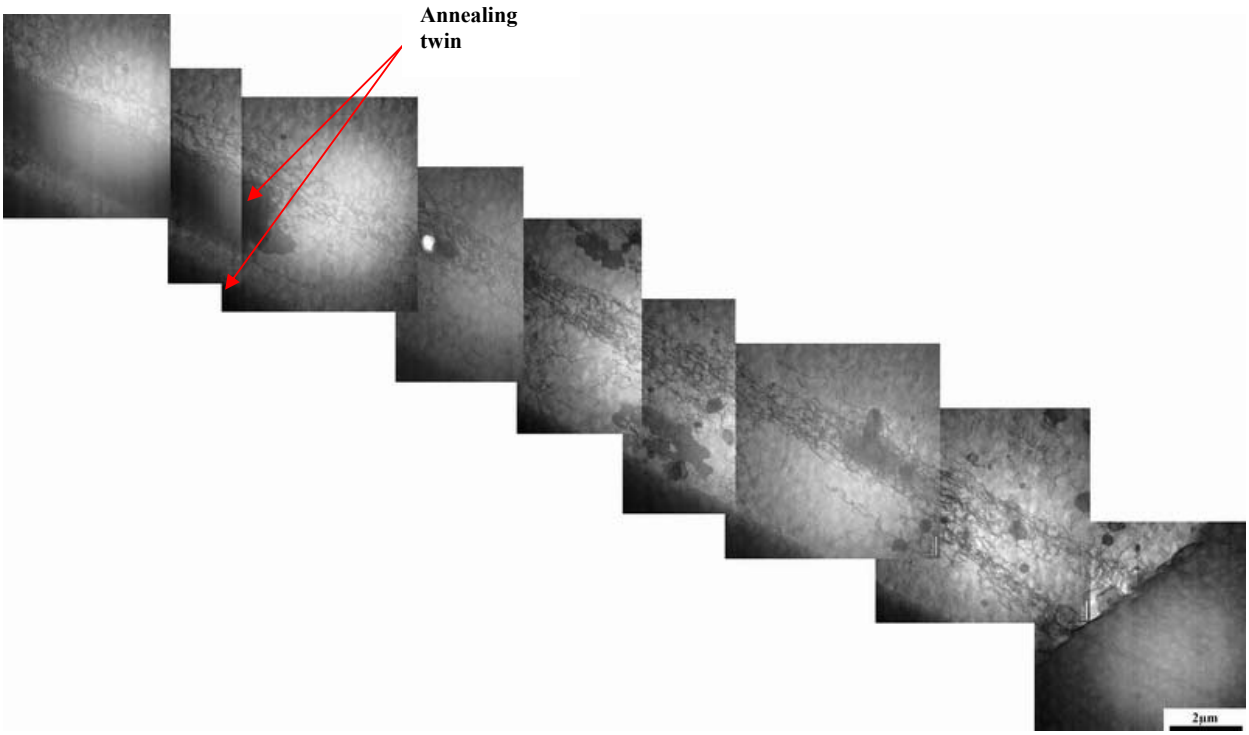

(a)

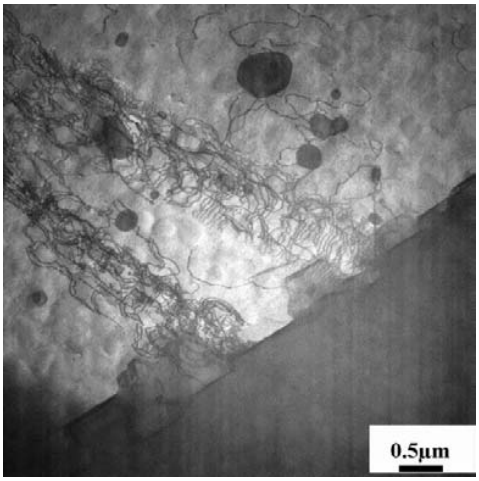

(b)

Figure 11. Localization of cyclic plastic deformation within a slip band, (a) overview of the slip band, (b) detailed structure of the slip band.

Conclusions

The fatigue behavior of the nickel-based superalloy René 88DT was studied at 593°C in the fatigue lifetime regime up to 10^9 cycles by ultrasonic fatigue. In the testing stress range, all fatigue cracks initiated internally. Critical microstructural features associated with fatigue crack initiation and the early stage of small crack propagation were revealed by combining serial sectioning, quantitative fractographic analysis and OIM.

Most fatigue failures originate at large favorably oriented grains. Fatigue cracks initiated and subsequently propagated along {111} slip planes oriented for maximum resolved shear stress. The presence of annealing twin boundaries may contribute to fatigue crack initiation processes. These observations indicate that the high cycle fatigue life could be improved by reducing or eliminating large grains.

Acknowledgements

This work was supported by the Air Force Office of Scientific Research (F49620-03-1-0069, Dr. J.Tiley, Program Manager) and DARPA (Dr. Leo. Christoudolou, program manager).

References

[1]. ENSIP, Engine Structural Integrity Program Handbook, http://engineeringwpafb.af.mil/corpusa/handbook/mh1783/mh1783.pdf, 2002. 135

[2]. H. Mughrabi, "Specific features and mechanisms of fatigue in the ultrahigh-cycle regime", *International Journal of Fatigue*, 28 (2006), 501-508.

[3]. S.D. Antolovich and B. Lerch. "Cyclic deformation and fatigue in Ni-base alloy", *Superalloys, Supercomposites and Superceramics*, ed. John K. Tien and Thomas. Caufield, (New York, NY: Academic Press, 1989), 363-411.

[4] E.S. Huron and P.G. Roth, "The influence of inclusions on low cycle fatigue life in a P/M nickel-base disk superalloy", *Superalloys 1996*, ed. R.D. Kissinger, D.J. Deye, D.L. Anton, A.D. Cetel, M.V. Natahal, T.M. Pollock and D.A. Woodford, (Warrendale, PA: TMS, 1996), 359-367.

[5]. A. Debussac, "Prediction of the competition between surface and internal fatigue crack initiation in PM alloys', *Fatigue & Fracture of Engineering Materials and Structures*, 17 (11) (1994), 1319-1325.

[6]. F. E. Organ and M. Gell, "The effect of frequency on the elevated temperature fatigue of a nickel-base superalloy", *Metallurgical Transactions*, 2 (1971), 943-952.

[7]. C.H. Wells and C.P. Sullivan "The low-cycle fatigue characteristics of a Nickel-base superalloy at room temperature", *Transactions of the ASM*, 57 (1964), 841-855.

[8]. J.C Healy, L. Grabowski and C.J. Beevers, "Monitoring fatigue of a nickel-base superalloy at positive and negative stress ratios using an optical system", *Fatigue & Fracture of Engineering Materials & Structures*, 15 (1992), 309-321.

[9]. K. Li, N.E. Ashbaugh and A.H. Rosenberger, "Crystallographic initiation of nickel-base superalloy IN 100 at RT and 583 under low cycle fatigue conditions", *Superalloys 2004,* ed. K.A. Greeen, H. Harada, T.E. Howason, T.M. Pollock, R.C. Reed, J.J. Schirra and S. Walston, (Warrendale, PA: TMS, 2004), 251-258.

[10]. D. L. Davidson, R. G. Tryon, M. Oja, R. Matthews and K. S. Ravi Chandran, "Fatigue Crack Initiation in Waspaloy at 20 °C", *Metallurgical and Materials Transactions A*, 38 (2007), 2214-2225.

[11]. D. L. Davidson, "The effect of similarly oriented grains (a supergrain) on fatigue crack initiation characteristics of clean materials", *Fourth International Conference on Very High Cycle Fatigue*, ed. J. E. Allison, J.W. Jones, J.M. Larson and R.O. Ritchie, (Warrendale, PA: TMS, 2007), 23-28.

[12]. H. Mayer. "Fatigue crack growth and threshold measurements at very high frequencies", *International Materials Reviews*, 44 (1999), 1-34.

[13]. D.D. Krueger, R.D. Kissinger and R.G. Menzies. "Development and introduction of a damage tolerant high temperature Nickel-Base Disk Alloy, Renee 88DT", *Superalloys 1992*, ed. S.D.Antolovich, (Warrendale, PA: TMS-AIME,1992), 277-286.

[14]. A. Shyam, C.J. Torbet, S.K. Jha, J.M. Larsen, M.J. Caton, C.J. Szczepanski, T.M. Pollock, J.W. Jones. Development of ultrasonic fatigue for rapid, high temperature fatigue studies in turbine materials. *Superalloys 2004,* ed. K.A. Greeen, H. Harada, T.E. Howason, T.M. Pollock, R.C. Reed, J.J. Schirra and S. Walston, (Warrendale, PA: TMS, 2004), 259-268.

[15]. Jiashi Miao, T.M. Pollock, and J.W. Jones."Very high cycle fatigue behavior of nickel-based superalloy René 88DT at 593 °C", *Fourth International Conference on Very High Cycle Fatigue*, ed. J. E. Allison, J.W. Jones, J.M. Larson and R.O. Ritchie, (Warrendale, PA: TMS, 2007), 445-450

[16]. M.J. Caton, S.K. Jha, A.H. Rosenberger and J.M. Larson. "Divergence of mechanisms and the effect on the fatigue life variability of Rene 88DT", *Superalloys 2004,* ed. K.A. Greeen, H. Harada, T.E. Howason, T.M. Pollock, R.C. Reed, J.J. Schirra and S. Walston, (Warrendale, PA: TMS, 2004), 305-312.

[17]. N. Thompson, N. Wadsworth and N. Louat, "The origin of fatigue fracture in copper", *Philosophical Magazine*, 1 (1956), 113 – 126.

[18]. R.C. Boettner, J.A. McEvily, Jr and Y.C. Liu, "On the formation of fatigue cracks at twin boundaries", *Philosophical magazine*, 10 (1964), 95-106

[19]. A. Heinz and P. Neumann, "Crack initiation during high cycle fatigue of an austenitic steel", *Acta Metallurgica et Materialia*, 38 (1990), 1933-1940.

[20]. T.C. Lee, I.M. Robertson, and H.K. Birnbaum, "An In Situ transmission electron microscope deformation study of the slip transfer mechanisms in metals" *Metallurgical and Materials Transactions A*, 21 (1990), 2437-2447.

[21]. L. Lanes and C. Laird, "the role of annealing twin boundaries in the cyclic deformation of f.c.c materials". *Materials science and engineering A*, 157 (1992), 21-27.